

Measuring Basaltic Flow Viscosity From Crustal Thickness

A. M. Harburger (*amh135@pitt.edu*) and M. S. Ramsey (*mramsey@pitt.edu*)

Department of Geology and Planetary Science, University of Pittsburgh, Pittsburgh PA 15260



INTRODUCTION

Cooling of basaltic lava flows quickly produces a glassy crust that dramatically affects the thermal infrared (TIR) emitted energy from its surface. As the crust thickens it also impacts the development and frequency of flow folding, which has been used as a proxy for composition and crustal thickness. To better understand this TIR effect and to develop an approach to remotely monitor crustal growth and viscosity, TIR camera (FLIR S40) camera data at 30 Hz have been acquired of an actively folding and cooling basalt flow at Kilauea, Hawaii (Figure 1). Because the viscosity ratio between the surface and the interior of the flow can be related to crustal thickness and fold wavelength, it becomes possible to determine either the variation in viscosity or the crust thickness as the flow cools. We have performed these measurements for the first time on basaltic pahoehoe toes during the first few minutes following emplacement (Figures 2 & 3).



Figure 1. Satellite image composite of the Big Island of Hawaii, showing location of Kilauea volcano.



Figure 2. Pahoehoe toe emplacement showing initial crustal folds (2 meter viewing distance).



Figure 3. Actively-inflating basalt flows at the pad-scale with the FLIR camera in foreground.

APPROACH AND METHODOLOGY

FLIR measurements were made on 19 May 2010 at a distance of 2 m (relative humidity = 32%, ambient air temperature = 38.9°C). All infrared image data were corrected for atmospheric parameters and before extraction of calibrated surface temperatures. The TIR data were acquired at 30 frames per second in order to capture the details of folding, cooling, and spatial patterns at different stages of crustal formation. The video data were then analyzed using ThermaCAM Research Professional 2.7 for temperature and folding scales. These revealed a distinct trend in wavelength, which was used to determine the crust thicknesses and viscosity.

RESULTS AND DISCUSSION

As the lava began to cool and detectable crusts formed, first-generation folds (L_1) appeared. As the lava continued to flow and cool, these folds were incorporated into larger second-generation folds (L_2) as can be seen in Figure 4. The brightness temperature for various transects were exported (Figure 5) and resemble the larger-scale folding patterns of emplaced flows (Figure 6).

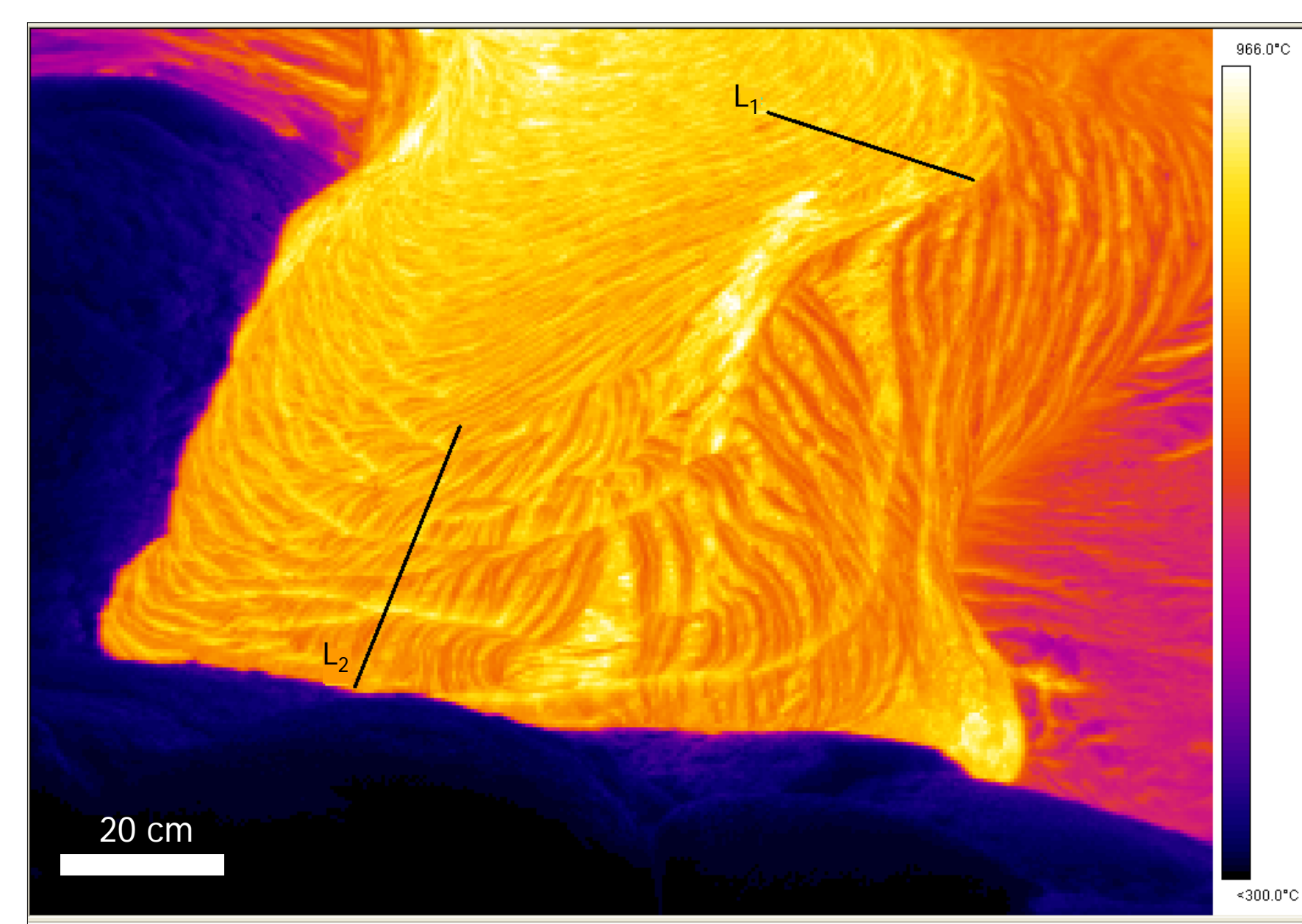


Figure 4. Single frame of the FLIR video data, showing transects L_1 and L_2 .

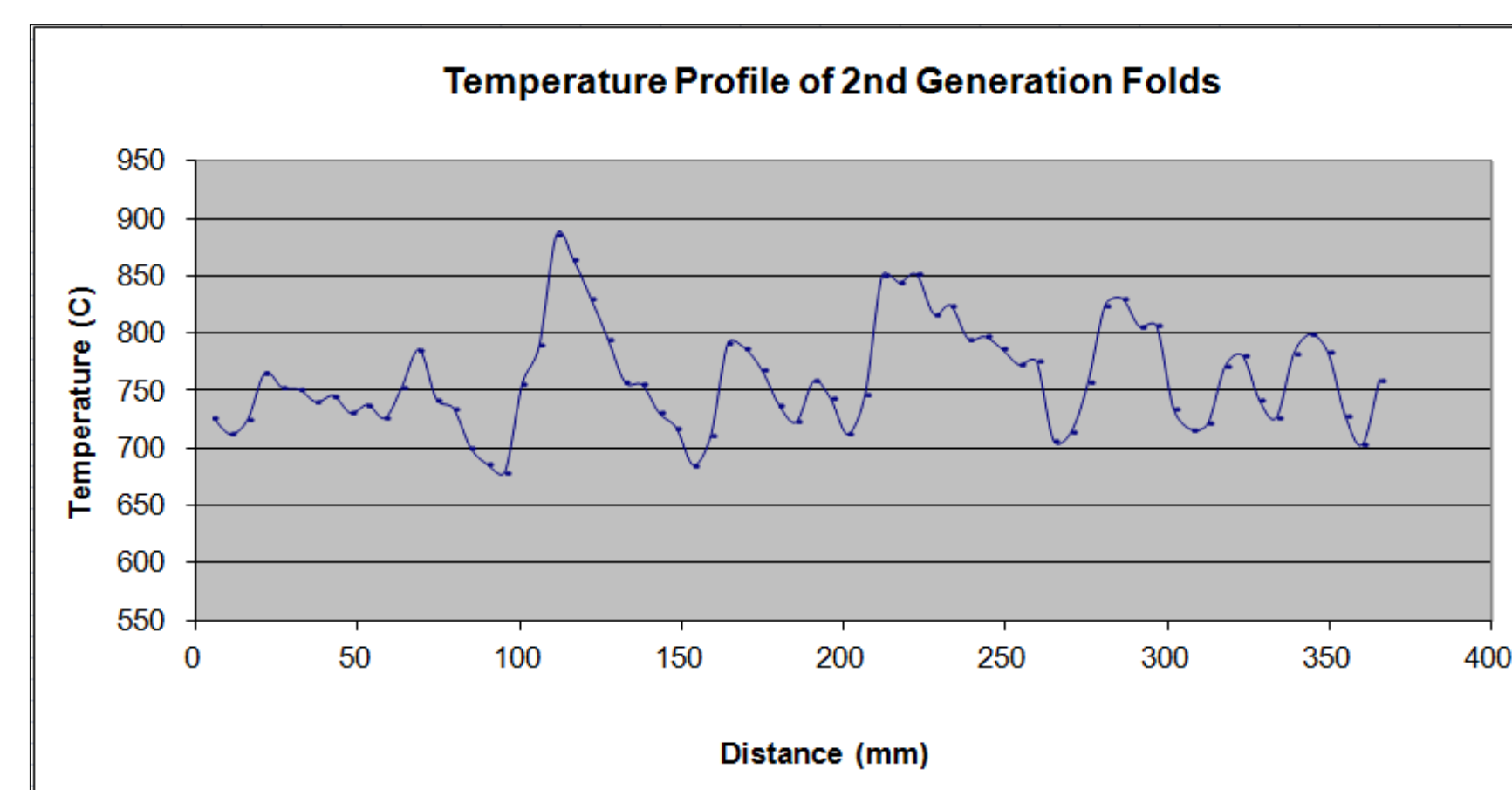


Figure 5. Plot of extracted FLIR temperature along transect L_2 .



Figure 6. Cooled basalt flows displaying first and second generation folding patterns, from Gregg et al. (1998).

Crust thicknesses were estimated based on samples collected in the field, and viscosities calculated using the equation $h=(1/\gamma) \ln R$, where $\gamma = 1/L_d$, $R = (\eta_o / \eta_i)$, h = crust thickness, L_d = dominant wavelength, η_o = surface viscosity, and η_i = interior viscosity of basalt. after Gregg et al. [1998]

In all stages of cooling two dominant folding wavelengths were found for each fold generation.

	L_1	L_2
Wavelength	21.2 mm, 31.8 mm	68.9 mm, 84.8 mm
Temperature	788°C	761°C
Crust thickness, h	1 mm	10 mm
Surface viscosity, η_o	1125.5 Pa·s ± 26.6	1140.7 Pa·s ± 15.6

RESULTS AND DISCUSSION

After the first and second generation fold calculations were made, the L_1 folds were further subdivided (Figure 7). Where the temperature patterns of the L_1 folds were analyzed, they displayed similar folding patterns, but on a much smaller scale (Figure 8). A schematic image of the multiple fold generations resembles the progression from small scale L_1 folds to larger L_3 folds (Figure 9).

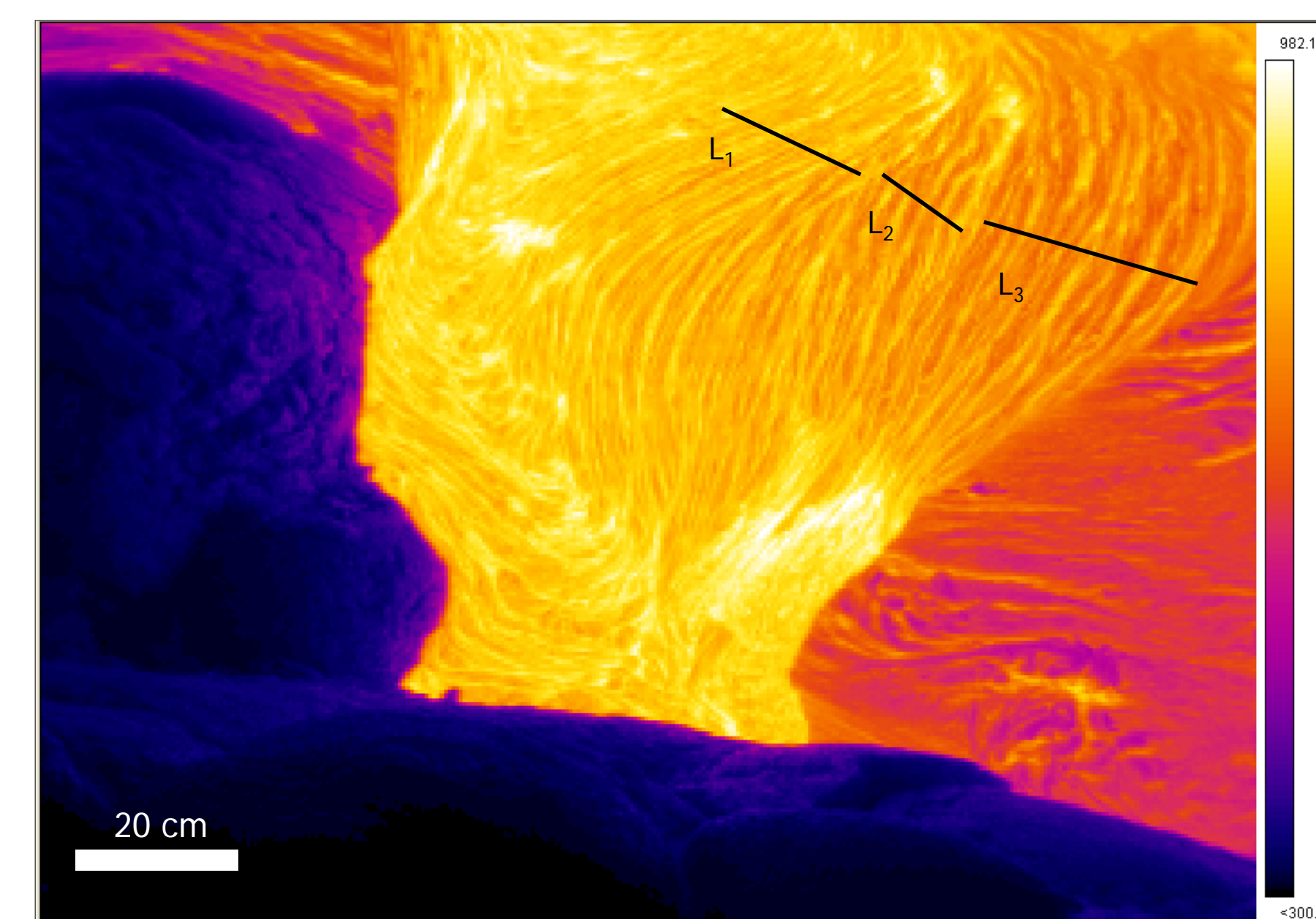


Figure 7. Single frame of the FLIR video data showing the first generation folds subdivided into L_1 , L_2 , and L_3 .

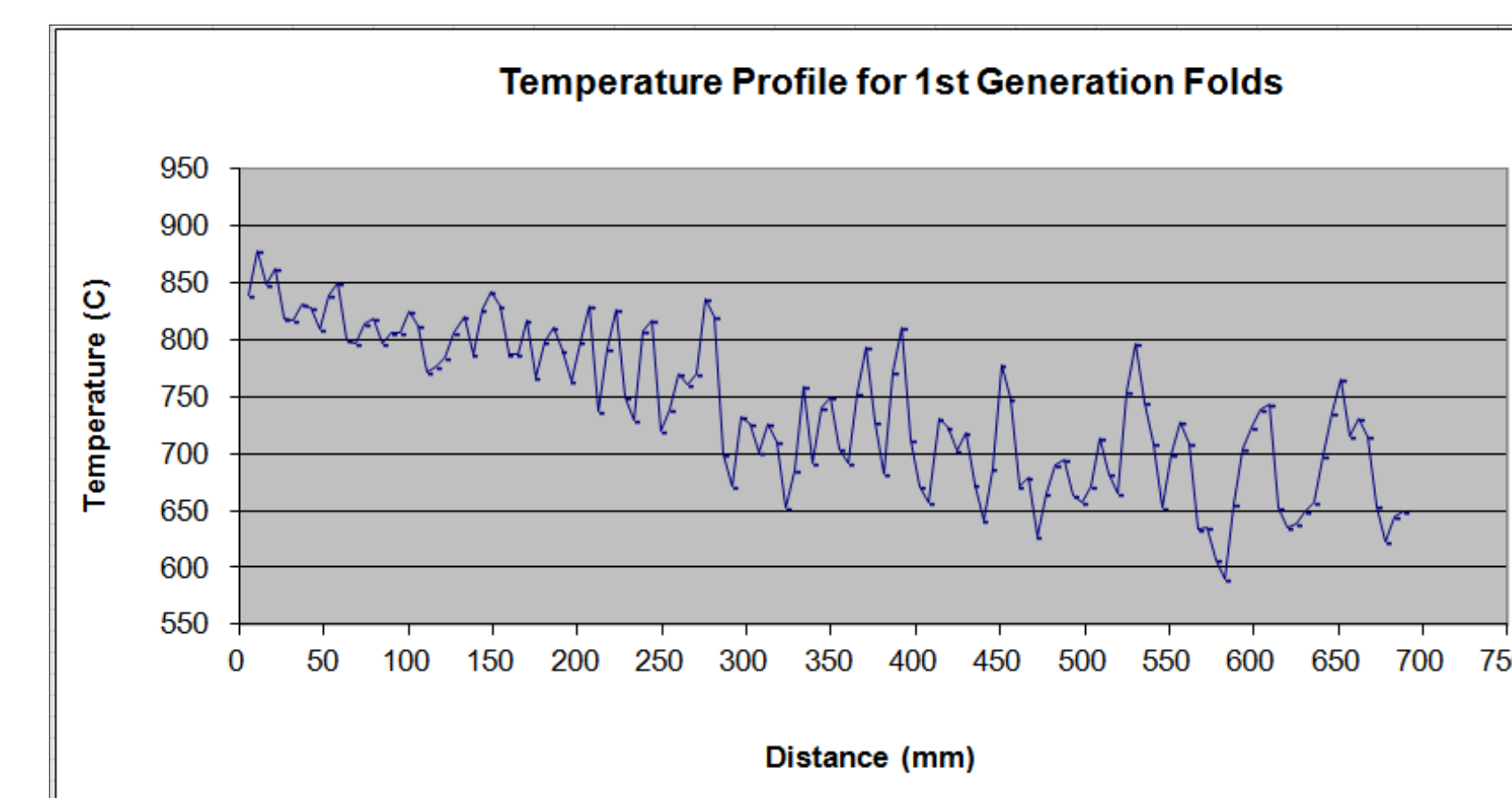


Figure 8. Plot of extracted FLIR temperature along transect L_1 .

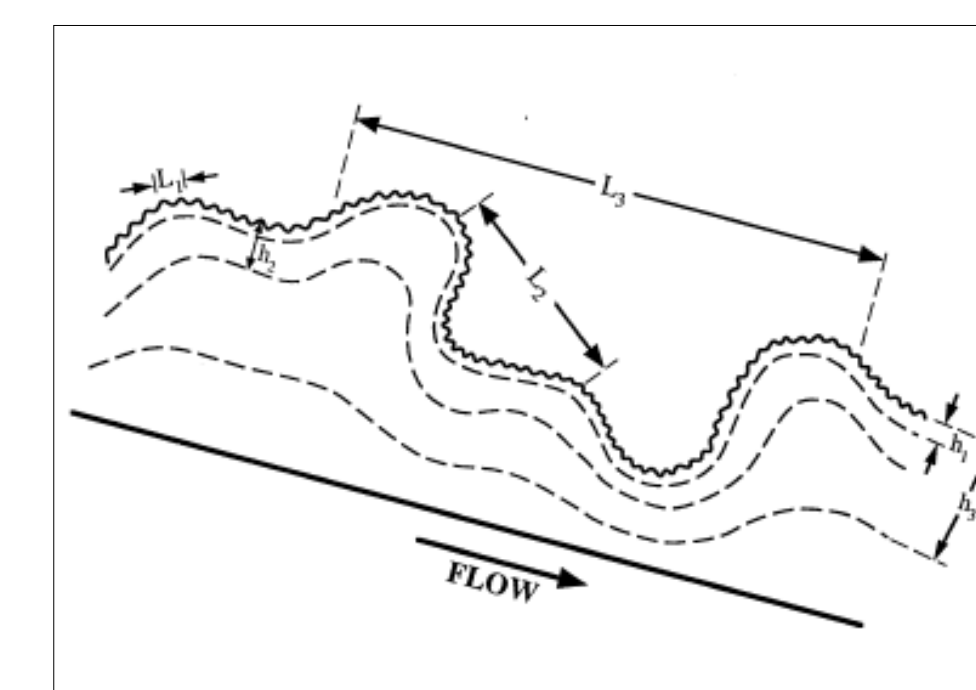


Figure 9. Schematic diagram of the folding process showing increasing crust thicknesses, from Gregg et al. (1998).

	L_1	L_2
Wavelength	10.6 mm, 15.9 mm	31.8 mm, 37.1 mm
Temperature	802°C	768°C
Crust thickness, h	1 mm	3 mm
Surface viscosity, η_o	1081.9 Pa·s ± 17.0	1091.7 Pa·s ± 7.3

At the very initial stage of folding, L_1 is 10.6 mm and 15.9 mm and L_2 is 31.8 mm and 37.1 mm. If $\Lambda = L_2 / L_1$, where Λ is a function of crust cooling and flow shortening, then $\Lambda = 2.6 \pm 0.3$.

At a slightly later stage, cooling results in the younger fold L_1 being 21.2 mm and 31.8 mm and L_2 is 68.9 mm and 84.8 mm therefore, $\Lambda = 3.0 \pm 0.3$.

CONCLUSIONS AND ONGOING RESEARCH

By analyzing high speed thermal infrared images of basaltic pahoehoe flow emplacement, the initial formation of the glassy crusts and the temperature of crust at fold initiation were documented. Further, multiple fold generations and folding dynamics were easily identified at multiple scales for every dominant wavelength. These folds were categorized in two discrete sections with the first exhibiting fold wavelengths between 21 - 84 mm, which resulted in crustal viscosities of 1125.5 Pa·s ± 26.6 and 1140.7 Pa·s ± 15.6. If the first generation folds were further subdivided, they exhibited fold wavelengths between 10 - 37 mm, with crustal viscosities of 1081.9 Pa·s ± 17.0 and 1091.7 Pa·s ± 7.3.

Additionally, the ratio (Λ) of the second generation wavelength, L_2 , to the first generation wavelength, L_1 , for basalt was calculated to be 5.1 ± 1.1 . This is approximately two times larger than the value shown in Gregg et al. (1998). As a result, this wavelength ratio as basalt is forming an initial crust is more closely related to the Λ values for dacite and rhyolite (Figure 10). Therefore, folding (and crust formation) at this early stage is dominated by heat loss rather than compression or flow thickening. With time and increasing crustal thickness, basalt flows become more insulated and compression becomes the primary mechanism controlling fold formation and spacing.

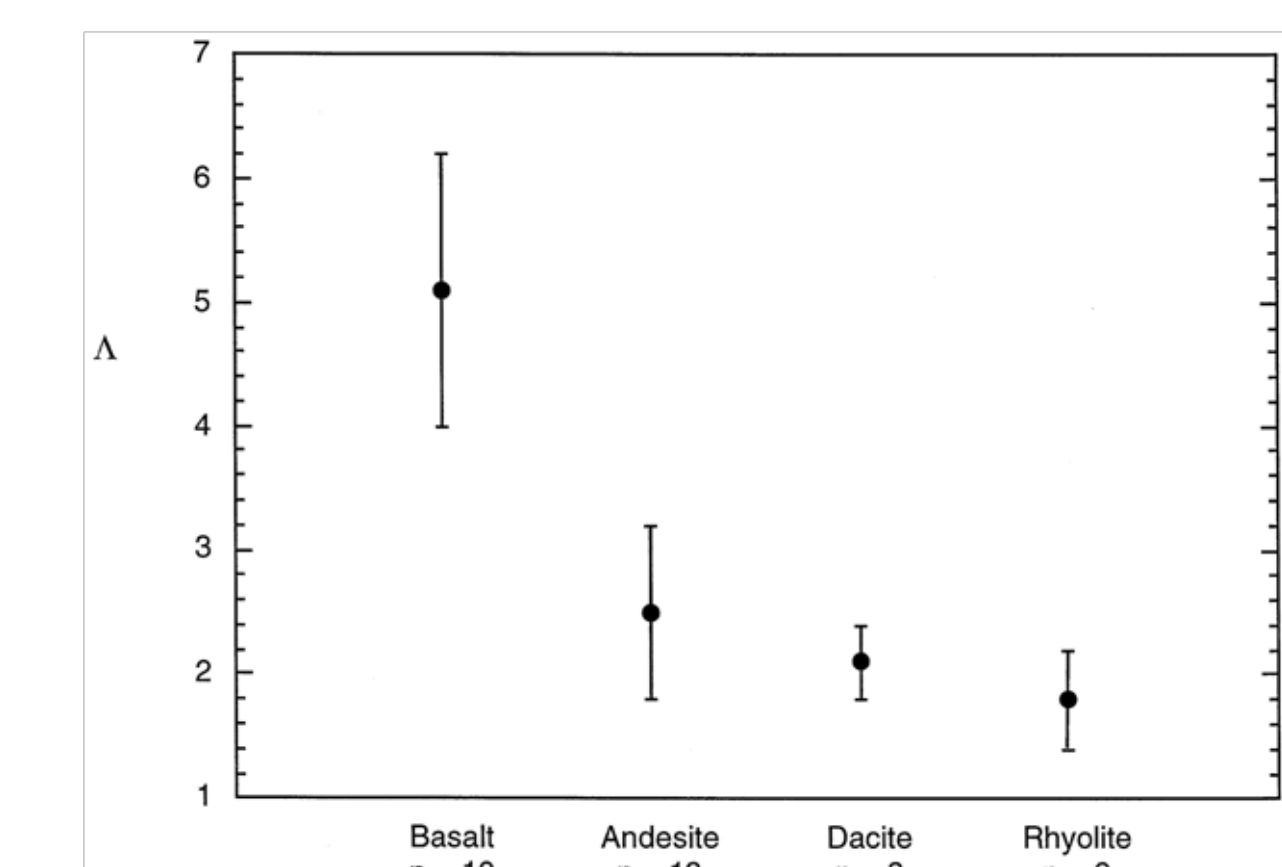


Figure 10. The relation between the ratio Λ and terrestrial lava flows: n indicates the number of flows measured for each composition (note the difference of basalt from the other compositions, from Gregg et al. (1998)).

Future work will entail combining these findings with velocity maps of the flows and cooling curves of the crust to further analyze the rheological and thermal properties of pahoehoe toes during emplacement. These measurements are critical in order to further constrain and model the thermal emission from these flows. The results could be applied to more accurately estimate lava flow cooling, eruptive environments, and composition.

ACKNOWLEDGEMENTS

This work was funded by the National Science Foundation (grant number EAR-1019558). The authors would like to thank the Hawaii Volcano Observatory (Matt Patrick and Mike Poland), as well as Ken Hon and Tracy Gregg for their assistance.

REFERENCES

- [1] Gregg, T.K.P., Fink, J.H., Griffiths, R.W., 1998. Formation of multiple fold generations on lava flow surfaces: influence of strain rate, cooling rate, and lava composition. *Journal of Volcanology and Geothermal Research* 80, 281-292. [2] Ball, M., Pinkerton, H., Harris, A.J.L., 2008. Surface cooling, advection and the development of different surface textures on active lavas on Kilauea, Hawaii. *Journal of Volcanology and Geothermal Research* 173, 148 - 15. [3] Fink, J.H., Fletcher, R.C., 1978. Ropy pahoehoe: Surface folding of a viscous fluid. *Journal of Volcanology and Geothermal Research* 4, 151-170. [4] Sato, H., 2005. Viscosity measurement of subliquidus magmas: 1707 basalt of Fuji volcano. *Journal of Mineralogical and Petrological Sciences* 100, 133-142.